Activation of endoplasmic reticulum stress and unfolded protein response in congenital factor VII deficiency

Elisabeth Andersen[1,2,3], Maria Eugenia Chollet[1,2], Christiane Filion Myklebust[1,2], Mirko Pinotti[4], Francesco Bernardi[4], Ampaiwan Chuansumrit[5], Ellen Skarpen[6], Per Morten Sandset[1,2,3], Grethe Skretting[1,2].

[1]Department of Haematology and [2]Research Institute of Internal Medicine, Oslo University Hospital, Oslo, Norway; [3]Institute of Clinical Medicine, University of Oslo, Oslo, Norway; [4]Department of Life Sciences and Biotechnology and LTTA Centre, University of Ferrara, Italy; [5]International Hemophilia Training Center, Ramathibodi Hospital, Mahidol University, Bangkok, Thailand; [6]Core Facility for Advanced Light Microscopy, Institute for Cancer Research, Oslo University Hospital, Norway.

Running title: ER stress in FVII deficiency

Corresponding author:

Senior Scientist Grethe Skretting
Research Institute of Internal Medicine
Oslo University Hospital Rikshospitalet
Box 4950 Nydalen, NO-0424 Oslo, Norway.
Tel.: +47 90887269, Fax: +47 23073362
E-mail: grethe.skretting@medisin.uio.no

Funding

The study was supported by grants from the South-Eastern Norway Regional Health Authority.

Summary

Congenital factor (F) VII deficiency is a bleeding disorder caused by a heterogeneous pattern of mutations in the *F7* gene. Protein misfolding due to mutations is a strong candidate mechanism to produce the highly represented type I FVII deficiency forms, characterized by a concomitant deficiency of FVII antigen and activity. Misfolded proteins can accumulate within the endoplasmic reticulum (ER) causing ER stress with subsequent activation of the unfolded protein response (UPR). So far, there is limited data on this important issue in FVII deficiency. In this study, we chose as candidate FVII model mutations, the p.Q160R, p.I289del and p.A354V-p.P464Hfs, which are all associated with severe to moderate type I FVII deficiency. *In vitro* expression of the recombinant (r) mutants rFVII-160R, rFVII-289del or rFVII-354V-464Hfs, that are characterized by either amino acid substitution, deletion, or by an extended carboxyl terminus, demonstrated inefficient secretion of the mutant proteins, probably caused by intracellular retention and increased association with ER chaperones. Both ER stress and UPR were activated following expression of all FVII mutants, with the highest response for rFVII289del and rFVII354V-464Hfs. These data unravel new knowledge on pathogenic mechanisms leading to FVII deficiency, and support the investigation of pharmaceutical modulators of ER stress and UPR as therapeutic agents.

Keywords: Factor VII deficiency; endoplasmic reticulum stress; unfolded protein response.

Introduction

Coagulation factor (F) VII is a zymogen single-chain vitamin K-dependent glycoprotein comprising a gamma-glutamic acid (GLA) domain, followed by two epidermal growth factor (EGF)-like domains, an activation domain, and a catalytic domain (1). The protein is synthesized by the liver and circulates in plasma at a concentration of about 0.5 µg/ml (2). Upon vascular damage, circulating FVII binds to its cofactor tissue factor (TF), and is then immediately activated to a two chain protease (FVIIa) (3). The TF/FVIIa catalytic complex is the physiological trigger of the coagulation cascade (4).

Congenital FVII deficiency is a rare, autosomal recessive bleeding disorder caused by *F7* gene mutations and is usually subdivided into two forms: type I and type II (5). Type I deficiency is characterized by a concomitant reduction of both FVII antigen (FVII:Ag) and FVII activity (FVII:C). Amino acid substitutions or deletion/insertion that affect the three-dimensional protein structure may cause misfolding. Thus, protein misfolding represents a key disease-causing mechanism (6). Several candidate *F7* mutations might be pathogenic through this mechanism. Patients with the missense mutation p.Q160R (formerly named Q100R) located in the second EGF-domain manifest with bleeding episodes (7). The mutation p.I289del (formerly named del229I) is a one-residue deletion in the catalytic domain of the FVII protein and has been identified in a newborn suffering from central nervous system bleeding at birth and undetectable FVII:Ag in plasma (Chollet et. al., manuscript submitted for publication). Another mutation is p.A354V-p.P464Hfs (formerly named A294V-11125delC) that is characterized by being a missense mutation in the FVII catalytic domain and also by a cytosine deletion at position 11125 responsible for a frameshift at the C-terminal codon 464 resulting in an extra 28 amino acid tail (8). This double mutation is associated with diverse clinical phenotypes ranging from asymptomatic to severe due to reduced FVII:Ag and FVII:C (9).

The secretory defects observed in these FVII deficiency patients can be attributed to a misfolded mutant molecule. Prolonged accumulation of misfolded proteins within the ER may cause ER stress and subsequent activation of a signalling pathway termed the unfolded protein response (UPR) (10). ER stress has been implicated in the pathogenesis of many diseases caused by the misfolding of cellular proteins (11) and a link between misfolded coagulation factors and ER stress has been described (12, 13). Furthermore, it was previously shown that expression of recombinant human FVIII engaged the UPR pathway, and that induction of ER stress by glucose deprivation led to increased expression of the *F7* gene through activating transcription factor 4 (ATF4) (14, 15). However, these responses have been poorly investigated in relation to FVII deficiency. In the present study, we therefore used an *in vitro* cell culture model to examine the intracellular fate of the recombinant mutants rFVII-160R, rFVII-289del and rFVII-354V-464Hfs. We found that all the rFVII mutants were poorly secreted, most likely due to intracellular retention and prolonged association with folding chaperones in the ER. We also demonstrated an increased ER stress response and activation of the UPR in cells expressing the rFVII mutants. Expression of rFVII-289del and rFVII-354V-464Hfs generated the strongest responses concurrent with the severely reduced secretion of FVII:Ag from these cells.

Materials and methods

Cell cultures

The human embryonic kidney cell line HEK293 (American Type Culture Collection (ATCC), Rockville, MD, USA, CRL-1573), the Chinese hamster ovary cell line CHO-K1 (ATCC, CCL-61) and the hepatocellular carcinoma cell line Huh7 (ATCC, RCB 1366) were all maintained in Dulbecco's Modified Eagle's Medium (DMEM, Lonza Group Ltd., Basel, Switzerland) supplemented with 10% fetal bovine serum (FBS, GE Healthcare HyClone,

Utah, USA), 10 µg/ml vitamin K1 (Sigma Aldrich, Saint Louis, MO, USA) and 100 U/ml penicillin, 100 µg/ml streptomycin (Lonza) in a humidified atmosphere containing 5% CO_2 at 37 °C.

Expression vectors and transfection

pcDNA3-FVII wild-type (FVIIwt), pcDNA3-p.I289del, pcDNA3-p.A354V and pcDNA3-p.A354V-p.P464Hfs were generated as previously described (9, 16). pcDNA3-p.Q160R was generated using the Quick Change Site-Directed Mutagenesis II Kit (Agilent, Santa Clara, CA, USA) according to manufacturer's instructions using pcDNA3-FVIIwt as template with the forward primer 5'-CCCAGGAGTGTGAGTGTCCCGGGGG-3' and the reverse primer 5'-CCCCCGGGACACTCACACTCCTGGG-3'. All the sequences were validated by sequencing. Transient transfection of HEK293 cells was performed using Lipofectamine LTX with Plus reagent (Thermo Fisher Scientific, Waltham, MA, USA) diluted in Opti-MEM (Thermo Fisher Scientific) according to the manufacturer's protocol. The transfection efficiency was evaluated by co-transfection with pcDNA3.1(+)/CAT plasmid (Thermo Fisher Scientific). The activity of chloramphenicol acetyltransferase (CAT) was measured using CAT-ELISA Kit (Roche Applied Science, Indianapolis, IN, USA) and no statistical significant differences of CAT activity were observed in lysates from cells co-transfected with pcDNA3.1(+)/CAT and pcDNA3-FVIIwt, pcDNA3-p.Q160R, pcDNA3-p.I289del or pcDNA3-p.A354V-p.P464Hfs, respectively. To generate CHO-K1 cells stably expressing the rFVII mutants, cells were stably transfected with the corresponding plasmid constructs and grown in complete DMEM supplemented with 800 µg/ml G-418 (Thermo Fisher Scientific) for approximately three weeks. Positive clones were isolated and expanded and the clones with highest mRNA levels of FVII were used for further experiments. Stable cell lines were maintained in DMEM supplemented with 400 µg/ml G-418.

Expression studies on recombinant FVII mutants

Cell culture medium from cells with transient or stable expression of rFVII mutants was harvested and the cells were washed briefly with ice-cold phosphate-buffered saline (PBS) (Lonza) before lysis in RIPA buffer (Sigma-Aldrich) supplemented with 1x Halt Protease and Phosphatase Inhibitor Cocktail (Thermo Fisher Scientific). Cell lysates and cell culture medium were pre-cleared by centrifugation and total protein content in the lysates was measured using the BCA protein assay kit (Thermo Fisher Scientific). ELISA was performed on cell culture medium and lysates using the VisuLize™ Factor VII Antigen ELISA Kit (Affinity Biologicals, Ancaster, ON, Canada) according to the manufacturer's protocol. Colorimetric output was measured in a SpectraMax Plus spectrophotometer (Molecular Devices, Sunnyvale, CA, USA). FVII levels for the transiently transfected Huh7 cells were normalized by subtracting the endogenous FVII levels.

Analysis of protein half-life

CHO-K1 cells with stable expression of rFVII mutants were treated with the protein synthesis inhibitor cycloheximide (CHX) (80 µg/ml) (Sigma-Aldrich) in DMEM supplemented with 1% serum for various time-points to determine the intracellular half-lives of rFVIIwt and the rFVII mutants. Harvesting of cell lysates and measurement of intracellular levels of FVII:Ag and total protein were performed as described above.

Cignal reporter assays

Cignal reporter assays were performed on HEK293-cells with the Cignal ER-stress response element (ERSE) reporter (luc) kit or the Cignal activating transcription factor 6 (ATF6) reporter (luc) kit (both from SABiosciences, Frederick, MD, USA) using the manufacturer's protocol for transient co-transfection of expression vector and Cignal reporter assay. 48 h post-transfection, the cells were washed briefly with PBS at room temperature before lysis in 1x passive lysis buffer (Promega, Madison, WI, USA). 10 µl of the lysates were transferred to a white OptiPlate (Perkin Elmer, Waltham, MA, USA) and firefly and Renilla luciferase

activities were measured using the Dual-Luciferase Reporter Assay System on a Glomax 96 microplate luminometer (both from Promega). Firefly/Renilla ratios were used as raw data for the calculations to correct for transfection efficiency. For fold-change, the luciferase output was normalized against the non-inducible negative control, and the luciferase activity from cells expressing rFVIIwt was defined as 1.

Co-immunoprecipitation (Co-IP)

Transiently transfected HEK293 cells were washed twice with ice-cold PBS before lysis in lysis buffer (20 mM Hepes (pH 7.4), 150 mM NaCl, 1 mM EDTA, 1 mM EGTA, 1.0% Triton X-100, 0.5% deoxycholate (sodium salt) and 1x Halt Protease and Phosphatase Inhibitor Cocktail for 20 min on ice. Cell lysates were pre-cleared by centrifugation and total protein content in the lysates was measured (see section "Expression studies on recombinant FVII mutants"). 250µg of total protein from the lysates were incubated with magnetic beads (Dynabeads M-280 sheep anti-rabbit IgG, Thermo Fisher Scientific) coupled with anti-FVII antibodies (Abcam, Cambridge, UK) or negative control antibodies (normal rabbit IgG, Cell Signaling) overnight at 4°C. The beads were then washed with PBS supplemented with 0.1% BSA.). Bound complexes were eluted by boiling at 95°C in sample buffer containing 5% β-mercaptoethanol (Thermo Fisher Scientific). Complexes were analysed by Western blot analysis (See section "Western blot analysis").

Western blot analysis

Equal amounts of proteins from cell lysates of transiently transfected HEK293-cells were separated using SDS-PAGE with Mini-PROTEAN® TGX 10% precast gels (Bio-Rad, Hercules, CA, USA) before transfer onto a Sequi-Blot PVDF membrane or a nitrocellulose membrane (both from Bio-Rad) using the Mini Trans-Blot Electrophoretic Transfer Cell system (Bio-Rad). The membranes were incubated overnight at 4°C with primary antibodies against binding immunoglobulin protein (BiP), phospho-eukaryotic translation initiation

factor 2α (p-eIF2α), total eIF2α, activating transcription factor 4 (ATF4), β-actin, or α-tubulin (all from Cell Signaling Technology, Danvers, MA, USA). For chaperone analysis, a comparison between cells treated with the membrane-permeable crosslinker dithiobis (succinimidyl propionate) (DSP) and vehicle-treated cells was performed. FVII complexes were found to be stable to detergent-lysing conditions (data not shown). Consequently, no crosslinking reagent was used in the further studies. FVII:Ag levels were determined by ELISA and equal amounts of FVII protein were prepared in a non-reducing and non-denaturing sample buffer without heating before loading onto Mini-PROTEAN TGX 7.5% precast gels. SDS-PAGE was performed and transfer of the proteins was performed in transfer buffer with 0.01% SDS added to facilitate transfer of large complexes. The membranes were incubated overnight at 4 °C with primary antibodies against FVII, BiP or glucose regulated protein 94 (GRP94) (Cell Signalling Technology). For Co-IP analysis, eluates were loaded onto Mini-PROTEAN TGX 7.5% precast gels before transfer onto an Immun-Blot PVDF membrane (Bio-Rad). The membranes were incubated overnight at 4 °C with primary antibodies against FVII (R&D Systems, Minneapolis, MN, USA), BiP or GRP94. The membranes were washed and then incubated with the corresponding horseradish peroxidase (HRP)-conjugated secondary antibody (both from Santa Cruz Biotechnology, Da, TX, USA) for 1 h at room temperature. Co-IP membranes were incubated with the corresponding HRP-conjugated secondary antibody. The immune reactive proteins were developed using SuperSignal West Dura (Thermo Fisher Scientific) and chemiluminescent signals were quantified using an ImageQuant LAS-4000 mini Imager (GE Healthcare, Chicago, IL, USA).

Commentato [GS1]: Vi m,å sette dette inn i responsbrevet under punktet som omhandler data not shown, at vi har lagt til et nytt

Quantitative RT-PCR (qRT-PCR)

Total RNA was isolated from transiently transfected HEK293 cells 16, 24, and 48 h post-transfection using the MagMAX™-96 Total RNA Isolation Kit on a MagMAX™ Express-96

Deep Well Magnetic Particle Processor (both from Thermo Fisher Scientific). mRNA was reverse transcribed using the High capacity cDNA Reverse Transcription kit (Thermo Fisher Scientific). To analyze mRNA levels, qRT-PCR was performed using the TaqMan Gene Expression Master Mix on a 7900HT Fast Real-Time PCR system and the following Taqman assays: Hs01551992_m1 (F7), Hs00160195_m1 (phosphomannomutase 1, PMM1), Hs00427665_g1 (GRP94), Hs00169585_m1 (growth arrest and DNA damage inducible protein 34, GADD34), Hs00909569_g1 (ATF4), and Hs00358796_g1 (C/EBP homologous protein, CHOP) (all from Thermo Fisher Scientific). To determine the mRNA levels of spliced and unspliced X-box binding protein 1 (sXBP1 and uXBP1, respectively), SYBR green primers were designed that were specific to spliced (forward 5′-TGCTGAGTCCGCAGCAGGTG-3′) or unspliced (forward 5′-CTCAGACTACGTGCACCTCT-3′) XBP1 mRNA. The same reverse primer was used for both targets (reverse 5′-GCTGGCAGGCTCTGGGGAAG-3′). Glyceraldehyde 3-phosphate dehydrogenase (GAPDH) (forward primer 5′-AAGACGGGCGGAGAGAAACC-3′, reverse primer 5′-ACGACCAAATCCGTTGACTCC-3′) was used as endogenous control. SYBR green qRT-PCR was performed using the Power SYBR Green PCR Master Mix (Thermo Fisher Scientific) on a 7900HT Fast Real-Time PCR system. Cells treated with the ER stress inducer thapsigargin (2 μM for 4 h) were used as a positive control to evaluate the functionality of the primers. Relative sXBP1/uXBP1 ratio was increased ~5-fold in thapsigargin-treated cells (Suppl. Figure 1).

Treatment with UPR inhibitors

HEK293 cells were transiently transfected with pcDNA3-p.Q160R, pcDNA3-p.I289del or pcDNA3-p.A354V-p.P464Hfs. 24 hours post-transfection, the cells were treated with 1 or 2μM of the PERK inhibitor GSK2606414 (GSKi, Merck Millipore, Billerica, MA, USA), 1 or 2μM of the IRE1 inhibitor 4μ8C (Merck Millipore) or 200 or 400μM of the ATF6

cleavage inhibitor 4-(2-aminoethyl)benzenesulfonyl fluoride hydrochloride (AEBSF, Merck Millipore) for 48h in DMEM supplemented with 1% serum. Harvesting of cell lysates and measurement of intracellular levels of FVII:Ag and total protein were performed as described above (see section "Expression studies on recombinant FVII mutants").

Nomenclature

The human genome variation society (HGVS) nomenclature has been used throughout the manuscript since this nomenclature has become an international standard (http://varnomen.hgvs.org/).

Statistical analysis

The statistical analyses were performed using GraphPad Prism 7.0 (GraphPad Software, La Jolla, CA, USA). Comparisons between the rFVIIwt and the rFVII mutants were performed using one-way ANOVA. A p-value of ≤0.05 was considered as statistically significant.

Results

Reduced FVII levels in lysates and culture medium from cells expressing FVII mutants

Transiently transfected cells were harvested 48 h post-transfection and FVII levels were measured in cell lysates and culture medium. The intracellular levels of rFVII-160R, rFVII-289del and rFVII-354V-464Hfs were reduced by 30-50% relative to rFVIIwt. The secreted levels of rFVII-160R were reduced to 5% of rFVIIwt whereas the secreted levels of rFVII-289del and rFVII-354V-464Hfs were undetectable (Figure 1). To adjust for variations in cell number, the FVII levels were adjusted to the corresponding total protein content in the respective wells. To confirm that the mutants also failed to be secreted in liver cells, the FVII constructs were transiently transfected into Huh7 cells (Suppl. Figure 2) and similar results were obtained as with the non-expressing HEK293 cells.

To ensure that the differences in intracellular levels of the FVII mutants compared to FVIIwt were not due to differences in transcription, we next performed qRT-PCR after transfection. Similar amounts of F7 mRNA were found for all FVII mutants (Suppl. Figure 3).

Increased half-lives of FVII mutants

To examine the half-lives of the rFVII variants, the protein synthesis was arrested by CHX treatment. The intracellular FVII levels were assessed by ELISA at various time-points after the CHX treatment. The half-life of rFVIIwt was approximately 6 h. The half-life of rFVII-354V-464Hfs and rFVII-160R was ~16 and ~24 h, respectively, whereas the half-life of rFVII-289del was >24 h (Figure 2). The increased half-lives suggested intracellular retention of the rFVII mutants.

FVII mutants induce ER stress and activation of the UPR

To explore whether the indicated intracellular retention of the rFVII mutants caused ER stress, the cignal ERSE reporter (luciferase) system was used. A significant increase in luciferase activity was observed in cells expressing rFVII-160R (~1.2-fold), rFVII-289del (~1.4-fold) or rFVII-354V-464Hfs (~1.3-fold) compared to cells expressing rFVIIwt (Figure 3A).

To assess the transcriptional activity of the ER stress-regulated transcription factor ATF6, the ATF6 reporter (luciferase) reporter was employed. Transient expression of rFVII mutants rFVII-160R, rFVII-289del and rFVII-354V-464Hfs significantly increased luciferase activity, indicating activation ATF6 (Figure 3B).

The protein level of the ER stress associated chaperone BiP was examined and found to be increased in cells expressing the rFVII mutants compared to rFVIIwt (Figure 3C). The

increase in BiP was most prominent in the rFVII-354V-464Hfs expressing cells with a 2.5-fold induction compared to rFVIIwt (Figure 3C, right panel). Moreover, although not significant, the protein level of the UPR marker p-eIF2α was slightly increased in cells expressing the rFVII mutants relative to cells expressing the rFVIIwt (Figure 3D).

To explore UPR signalling in detail, mRNA levels of various UPR-related genes were examined by qRT-PCR. The relative ratio of sXBP1/uXBP1 was increased ~1.4-fold in rFVII-160R expressing cells, and ~1.6-fold in rFVII-289del- and rFVII-354V-464Hfs expressing cells (Figure 4A). Furthermore, the ratio was significantly higher in rFVII-354V-464Hfs and rFVII-289del expressing cells compared to rFVII-160R expressing cells. ATF4 mRNA was significantly increased in cells expressing rFVII-289del (~1.1-fold) and rFVII-354V-464Hfs (~1.2-fold), but not in cells expressing rFVII-160R (Figure 4B). Although not significant, Western blot analysis also demonstrated an increase in ATF4 protein in cells expressing rFVII-289del and rFVII-354V-464Hfs (Suppl. Figure 4). A ~1.2-fold induction of GRP94 mRNA was observed in cells expressing the rFVII mutants relative to rFVIIwt (Figure 4C). GADD34 mRNA levels were increased only in the rFVII-354V-464Hfs expressing cells (1.2-fold) (Figure 4D). CHOP mRNA levels were found to be increased by approximately 1.2-, 1.3-, and 1.6-fold in cells expressing rFVII-160R, rFVII-289del and rFVII-354V-464Hfs, respectively (Figure 4E). CHOP mRNA levels were significantly higher in rFVII-354V-464Hfs- and rFVII-289del expressing cells compared to rFVII-160R. Furthermore, the CHOP mRNA levels were significantly higher in rFVII-354V-464Hfs expressing cells compared to rFVII-289del expressing cells.

To assess the functional role of each of the arms of the UPR and their impact on biosynthesis of rFVII mutants, inhibitors of either PERK (GSKi), IRE1 (4μ8C) or activated ATF6 (AEBSF) were utilized. To test for the inhibitory effect of GSKi, protein levels of p-eIF2α were assessed by Western blot analysis. GSKi-treatment was found to reduce p-eIF2α

levels by XX% compared to non-treated cells (Suppl. Figure 5). To test for the inhibitory effect of 4μ8C on IRE1α, sXBP1 and uXBP1 mRNA levels were assessed by SYBR green qRT-PCR. Treatment with 1 or 2 μM 4μ8C was found to reduce the relative sXBP1/uXBP1 ratio by approximately 40 and 60%, respectively, compared to non-treated cells (Suppl. Figure 6). The inhibitory effect of AEBSF was assessed by Cignal ATF6 reporter assay and treatment with 200 or 400 μM AEBSF was found to reduce the transcriptional activity of ATF6 by approximately 60 and 70%, respectively (Suppl. Figure 7). Inhibition of each arm of the UPR significantly increased the levels of rFVII-160R, rFVII-289del and rFVII-354V-464Hfs in cell lysates (Figure 9).

Commentato [EA2]: In progress

Increased association between ER chaperones and the FVII mutants

To examine whether the FVII mutants were retained in ER due to an excessive binding to chaperones, FVII-chaperone complexes were analysed in lysates from HEK293 cells transiently transfected to express the rFVII variants. Cell lysates with equal amounts of rFVII were resolved using SDS-PAGE under non-reduced conditions. Western blot analysis with antibody against FVII revealed several complexes with molecular weights of approximately 180-250 kDa, 320-380 kDa and >380 kDa (Figure 5A). The band intensities were strongest in lysates from cells expressing the rFVII mutants compared to rFVIIwt. When antibodies against various ER chaperones were used, the results indicated that both rFVIIwt and the rFVII mutants were complexed with GRP94 and BiP (94 and 78 kDa, respecetively, Figure 5B). However, the association between the rFVII mutants and the chaperones in the complexes was stronger than that of rFVIIwt (Figure 5C, D and E). The observed band of about 180-250 kDa could represent a protein complex consisting of FVII, GRP94 and BiP (approximately 224 kDa). Additionally, the band of approximately 320-380 kDa might indicate a complex consisting of multiple BiP molecules. The identity of the molecules in the

> 380 kDa complex remains to be determined. No bands representing FVII in complex with calnexin, calreticulin, PDI or GRP170 could be detected (data not shown). Co-IP and Western blot analysis confirmed the specific interaction of FVII with BiP and GRP94 (Figure 5F).

Discussion

While misfolding and altered intracellular processing of the naturally occurring FVII variants are the most likely mechanisms underlying type I FVII deficiency, these mechanisms have not been addressed so far. In the present study we therefore examined different types of *F7* mutations, exemplified by the p.Q160R, p.I289del and p.A354V-p.P464Hfs, using an *in vitro* cell culture model. The main findings from this study were reduced secretion of the FVII mutants as a result of intracellular retention due to excessive binding to ER chaperones. Additional results demonstrated that the intracellular retention caused ER stress and activation of the UPR.

We found that the levels of rFVII:Ag secreted into the cell culture medium from cells expressing the rFVII mutants were in accordance with the levels observed in plasma of the patients. In patients homozygous for the p.Q160R mutation, the FVII:Ag level was in the 10-28% range (7). Plasma levels in patients with the p.A354V-p.P464Hfs mutation are very low (median FVII:Ag 1.9%) (9), and in patients with the p.I289del mutation the FVII:Ag is undetectable (Chollet et al., manuscript submitted for publication). For some coagulation factor deficiencies an impaired secretion of the mutant protein due to ER retention (17, 18) has been demonstrated. In a previous study, rFVII-160R was shown to be localized to ER structures (19), and we have recently shown that rFVII-289del and rFVII-354V-464Hfs were retained in ER without reaching Golgi (Chollet et al., manuscript submitted for publication). The present study demonstrates increased half-lives of the rFVII mutants, indicating that the

reduced intracellular levels of the mutants were not due to reduced half-lives. The changes in intracellular protein levels could be explained by differences in degradation. However, when treating cells expressing rFVII-289del and rFVII-354V-464Hfs with lysosomal or proteasomal inhibitors, or an inhibitor of cysteine protease, calpain and proteasome, no changes in the intracellular FVII levels were observed (Chollet et al., manuscript submitted for publication). Additionally, a previous study showed that treatment with several inhibitors of protein degradation did not increase the intracellular levels of rFVII-160R (19).

Compared to the very low FVII:Ag levels in patients harbouring the p.A354V-p.P464Hfs mutation, patients with only the p.A354V mutation have average FVII:Ag levels of 52±11% (20) with a dysfunctional FVII affecting the interaction with other coagulation proteins (21). Correspondingly, when we measured the secreted level of FVII from cells transiently transfected to express rFVII-354V it was ~70% of the rFVIIwt level (Suppl. Figure 8). No differences in ER stress signalling were observed in the transiently transfected cells expressing rFVII-354V compared to rFVIIwt (Suppl. Figure 9). It has previously been shown that the frameshift mutation p.P464Hfs was associated with a marked reduction in FVII:C (22). This might indicate that in patients with the p.A354V-p-P464Hfs mutation, the p.P464Hfs in the C-terminal end of FVII could be responsible for the intracellular retention and increased ER stress elicited by this double mutation.

Retention and accumulation of proteins within the ER can disturb ER homeostasis and cause ER stress (23, 24). We observed increased levels of ER stress in cells expressing rFVII mutants compared to rFVIIwt, with the highest levels in cells expressing rFVII-289del and rFVII-354V-464Hfs. The FVII levels in lysates from cells expressing the rFVII mutants were lower than in lysates from rFVIIwt cells. Additionally, FVII levels in lysates from rFVII-289del- and rFVII-354V-464Hfs expressing cells were lower than in lysates from rFVII-160R expressing cells. Under conditions of ER stress, cells can repress translation through

the increased phosphorylation of eIF2α (25, 26) and we observed increased levels of p-eIF2α in cells expressing the rFVII variants compared to rFVIIwt. Thus, an overall reduction of protein synthesis as a result of ER stress could explain the decreased FVII levels in lysates from cells expressing the rFVII mutants.

ATF6 is an ER transmembrane protein that functions as a transcription factor activating transcription of genes involved in the UPR during ER stress. ATF6 transcriptional activity was found to be increased in cells expressing the rFVII mutants compared to rFVIIwt. XBP1 mRNA is induced by ATF6 and spliced by IRE1α in response to ER stress (27). An increased ratio of spliced versus unspliced XBP1 mRNA in cells expressing the rFVII mutants relative to rFVIIwt was observed, coinciding with a higher level of ER stress in these cells. The expression of GRP94 can be activated by various transcription factors including sXBP1 (28) and its mRNA level was increased in cells expressing the rFVII mutants relative to in cells expressing rFVIIwt. The basal expression of ATF4 is quite stable in cells, but its translation is preferentially induced by p-eIF2α (29). mRNA and protein levels of ATF4 were increased in cells expressing rFVII-289del and rFVII-354V-464Hfs, but not in cells expressing rFVII-160R. ATF4 is required for GADD34 induction and together they form a feedback-loop to resume protein translation during ER stress by dephosphorylating eIF2α (30). GADD34 was induced only in cells expressing rFVII-354V-464Hfs. The CHOP gene promoter contains binding sites for all of the major inducers of the UPR, including ATF4, ATF6 and XBP1 (31, 32). We found that CHOP mRNA levels were elevated in cells expressing the FVII mutants with the highest levels in cells expressing rFVII-354V-464Hfs. These results indicate that the increased ER stress observed in cells expressing rFVII-289del and rFVII-354V-464Hfs resulted in a stronger UPR response as demonstrated by the increased mRNA levels of UPR mediators. As compared with the FVII-160R, these variants are characterized by ample structural changes of FVII produced by the

deletion/insertion of one or several amino acid residues. Indeed, there is evidence that UPR is modulated differentially to various forms of ER stress (33, 34) and also according to severity and duration of the stress (35). A previous study showed that diminished engagement of the UPR enhanced the biosynthesis of coagulation factor FVIII (14). To study the impact on biosynthesis of rFVII mutants by UPR intervention, inhibitors of PERK (GSKi), IRE1α (4μ8C) or activated ATF6 (AEBSF) were utilized. Intracellular FVII:Ag levels were found to be significantly increased in response to treatment. Due to the decrease in total protein observed in treated cells most likely caused by toxicity issues, raw FVII:Ag levels were used in the calculation. However, the same trend in effect could be observed when relating to total protein content in each sample. Inhibition of PERK and IRE1α by GSKi and 4μ8C, respectively, moderately increased FVII:Ag levels in cell lysates (1.1 to 1.4-fold) compared to inhibition of activated ATF6 by AEBSF which increased intracellular FVII:Ag by 2 to 2.5-fold. AEBSF inhibits activation of ATF6 by inhibiting serine proteases in the Golgi apparatus responsible for cleavage of ATF6 to active ATF6. The present study show that the transcriptional activity of ATF6 was decreased by 50% in response to AEBSF-treatment. ATF6 can induce the promoter of genes regulated by glucose through ER stress response elements (ERSEs) (36) and thereby increase the expression of ER chaperones (37). Consequently, the effect of ATF6 inhibition on biosynthesis of rFVII might be caused by decreased expression of ER chaperones as was previously demonstrated by Brown et. al where BiP downregulation increased biosynthesis of FVIII (14), and Miao et al. where incorporation of a point-mutation within a putative BiP binding region of FVIII increased secretion (38). Therapeutic interventions that target molecules of the UPR and reduce ER stress are emerging (32, 39, 40). Examples are Salubrinal, a PERK antagonist shown to increase neuronal survival in a murine model of Parkinsons's disease (41), Bortezomib, an FDA-approved proteasomal inhibitor for treatment of multiple myeoloma (42) and chemical

Commentato [EA3]: I am afraid that the reviwers might ask to see expression levels of ER chaperones if I leave this sentence so I'm unsure of whether we should include it.

chaperones such as sodium phenylbutyrate (43) or Lumacaftor (VX-809) (44) both FDA-approved for treatment of urea cycle disorders and cystic fibrosis, respectively.

Previously, we demonstrated that the protein C (PC) mutant A267T had an excessive binding to ER chaperones compared to PCwt (13). Similar results have been reported for a FVII and a FIX mutant (45, 46). Our data indicates that rFVII, both wt and the mutants, formed complexes with chaperones in the ER. However, the rFVII mutants appeared to have a stronger association with the chaperones in the complex compared to rFVIIwt. We identified high molecular weight bands that could correspond to a protein complex consisting of FVII, GRP94 and BiP and, additionally, a complex that may correspond to FVII bound to multiple BiP molecules. The interaction of BiP or GPR94 with FVII was further supported by results from Co-IP. Indeed, clustering or multiple binding of chaperones has been shown to be kinetically favourable and may facilitate protein folding *in vivo* (47). Thus, prolonged interaction of rFVII-160R, rFVII-289del and rFVII-354V-464Hfs with ER chaperones could explain the decreased secretion.

In conclusion, our study demonstrates that the mutant proteins rFVII-160R, rFVII-289del and rFVII-354V-464Hfs were retained intracellularly due to an excessive binding to ER chaperones. The intracellular retention caused ER stress and activation of the UPR. All these events resulted in a reduced secretion of all three mutant FVII molecules from the cells. The major secretory defect observed *in vitro* is consistent with the clinical phenotypes associated with the p.Q160R, p.I289del and p.A354V-p.P464Hfs mutations. Treatment with inhibitors of the UPR was found to increase intracellular FVII levels. Insights into the intracellular processing and secretion of the rFVII mutants requires further studies, but is of great interest to uncover the possible therapeutic potential of these compounds since they could represent promising strategies to treat FVII deficiency specifically, and also deficiencies in vitamin K dependent coagulations factors in general.

Conflict of interest

The authors state that they have no conflict of interests.

Acknowledgements

The authors wish to thank Marie-Christine Mowinckel and Benedicte Stavik for their help with the ELISAs.

References

1. Hagen FS, Gray CL, O'Hara P, et al. Characterization of a cDNA coding for human factor VII. Proc Natl Acad Sci U S A 1986; 83: 2412-2416.

2. McVey JH, Boswell E, Mumford AD, et al. Factor VII deficiency and the FVII mutation database. Hum Mutat 2001; 17: 3-17.

3. Rao LV, Rapaport SI. Activation of factor VII bound to tissue factor: a key early step in the tissue factor pathway of blood coagulation. Proc Natl Acad Sci U S A 1988; 85: 6687-6691.

4. Mackman N. The role of tissue factor and factor VIIa in hemostasis. Anesth Analg 2009; 108: 1447-1452.

5. Girolami A, Bertozzi I, de Marinis GB, et al. Activated FVII levels in factor VII Padua (Arg304Gln) coagulation disorder and in true factor VII deficiency: a study in homozygotes and heterozygotes. Hematology 2011; 16: 308-312.

6. Valastyan JS, Lindquist S. Mechanisms of protein-folding diseases at a glance. Dis Model Mech 2014; 7: 9-14.

7. Kavlie A, Orning L, Grindflek A, et al. Characterization of a factor VII molecule carrying a mutation in the second epidermal growth factor-like domain. Thromb Haemost 1998; 79: 1136-1143.

8. Branchini A, Baroni M, Pfeiffer C, et al. Coagulationfactor VII variants resistant to inhibitory antibodies. Thromb Haemost 2014; 112.

9. Mariani G, Herrmann FH, Dolce A, et al. Clinical phenotypes and factor VII genotype in congenital factor VII deficiency. Thromb Haemost 2005; 93: 481-487.

10. Ma Y, Hendershot LM. The mammalian endoplasmic reticulum as a sensor for cellular stress. Cell Stress Chaperones 2002; 7: 222-229.

11. Yoshida H. ER stress and diseases. FEBS J 2007; 274: 630-658.

12. Malhotra JD, Miao H, Zhang K, et al. Antioxidants reduce endoplasmic reticulum stress and improve protein secretion. Proc Natl Acad Sci U S A 2008; 105: 18525-18530.

13. Tjeldhorn L, Iversen N, Sandvig K, et al. Protein C mutation (A267T) results in ER retention and unfolded protein response activation. PloS one 2011; 6: e24009.

14. Brown HC, Gangadharan B, Doering CB. Enhanced biosynthesis of coagulation factor VIII through diminished engagement of the unfolded protein response. J Biol Chem 2011; 286: 24451-24457.

15. Cronin KR, Mangan TP, Carew JA. Upregulation of the coagulation factor VII gene during glucose deprivation is mediated by activating transcription factor 4. PloS one 2012; 7: e40994.

16. Pinotti M, Toso R, Redaelli R, et al. Molecular mechanisms of FVII deficiency: expression of mutations clustered in the IVS7 donor splice site of factor VII gene. Blood 1998; 92: 1646-1651.

17. Tjeldhorn L, Iversen N, Sandvig K, et al. Functional characterization of the protein C A267T mutation: evidence for impaired secretion due to defective intracellular transport. BMC Cell Biol 2010; 11: 67.

18. Tanaka R, Nakashima D, Suzuki A, et al. Impaired secretion of carboxyl-terminal truncated factor VII due to an F7 nonsense mutation associated with FVII deficiency. Thromb Res 2010; 125: 262-266.

19. Hunault M, Arbini AA, Carew JA, et al. Characterization of two naturally occurring mutations in the second epidermal growth factor-like domain of factor VII. Blood 1999; 93: 1237-1244.

20. Herrmann FH, Wulff K, Strey R, et al. Variability of clinical manifestation of factor VII-deficiency in homozygous and heterozygous subjects of the European F7 gene mutation A294V. Haematologica 2008; 93: 1273-1275.

21. Toso R, Pinotti M, High KA, et al. A frequent human coagulation Factor VII mutation (A294V, c152) in loop 140s affects the interaction with activators, tissue factor and substrates. Biochem J 2002; 363: 411-416.

22. Arbini AA, Bodkin D, Lopaciuk S, et al. Molecular analysis of Polish patients with factor VII deficiency. Blood 1994; 84: 2214-2220.

23. Rutkowski DT, Kaufman RJ. A trip to the ER: coping with stress. Trends Cell Biol 2004; 14: 20-8.

24. Sitia R, Braakman I. Quality control in the endoplasmic reticulum protein factory. Nature 2003; 426: 891-894.

25. Iwawaki T, Hosoda A, Okuda T, et al. Translational control by the ER transmembrane kinase/ribonuclease IRE1 under ER stress. Nat Cell Biol 2001; 3: 158-164.

26. Brostrom CO, Brostrom MA. Regulation of translational initiation during cellular responses to stress. Prog Nucleic Acid Res Mol Biol 1998; 58: 79-125.

27. Yoshida H, Matsui T, Yamamoto A, et al. XBP1 mRNA is induced by ATF6 and spliced by IRE1 in response to ER stress to produce a highly active transcription factor. Cell 2001; 107: 881-891.

28. Marzec M, Eletto D, Argon Y. GRP94: An HSP90-like protein specialized for protein folding and quality control in the endoplasmic reticulum. Biochim Biophys Acta 2012; 1823: 774-787.

29. Harding HP, Novoa I, Zhang Y, et al. Regulated translation initiation controls stress-induced gene expression in mammalian cells. Mol Cell 2000; 6: 1099-1108.

30. Ma Y, Hendershot LM. Delineation of a negative feedback regulatory loop that controls protein translation during endoplasmic reticulum stress. J Biol Chem 2003; 278: 34864-34873.

31. Ma Y, Brewer JW, Diehl JA, et al. Two distinct stress signaling pathways converge upon the CHOP promoter during the mammalian unfolded protein response. J Mol Biol 2002; 318: 1351-1365.

32. Kim I, Xu W, Reed JC. Cell death and endoplasmic reticulum stress: disease relevance and therapeutic opportunities. Nat Rev Drug Discov 2008; 7: 1013-1030.

33. Hetz C. The unfolded protein response: controlling cell fate decisions under ER stress and beyond. Nat Rev Mol Cell Biol 2012; 13: 89-102.

34. DuRose JB, Tam AB, Niwa M. Intrinsic capacities of molecular sensors of the unfolded protein response to sense alternate forms of endoplasmic reticulum stress. Mol Biol Cell 2006; 17: 3095-3107.

35. Rutkowski DT, Kaufman RJ. That which does not kill me makes me stronger: adapting to chronic ER stress. Trend Biochem Sci 2007; 32: 469-476.

36. Yoshida H, Haze K, Yanagi H, et al. Identification of the cis-acting endoplasmic reticulum stress response element responsible for transcriptional induction of mammalian glucose-regulated proteins. Involvement of basic leucine zipper transcription factors. J Biol Chem 1998; 273: 33741-33749.

37. Lee AS. Mammalian stress response: induction of the glucose-regulated protein family. Curr Opin Cell Biol 1992; 4: 267-273.

38. Miao HZ, Sirachainan N, Palmer L, et al. Bioengineering of coagulation factor VIII for improved secretion. Blood 2004; 103(9): 3412-9.

39. Hetz C, Chevet E, Harding HP. Targeting the unfolded protein response in disease. Nat Rev Drug Discov 2013; 12: 703-719.

40. Kraskiewicz H, FitzGerald U. InterfERing with endoplasmic reticulum stress. Trends Pharmacol Sci 2012; 33: 53-63.

41. Colla E, Coune P, Liu Y, et al. Endoplasmic reticulum stress is important for the manifestations of alpha-synucleinopathy in vivo. J Neurosci 2012; 32: 3306-3320.

42. United States Food and Drug Administration. Hematology/Oncology (Cancer) Approvals & Safety Notifications. http://www.fda.gov/Drugs/InformationOnDrugs/ApprovedDrugs/ucm279174.htm.

43. Cortez L, Sim V. The therapeutic potential of chemical chaperones in protein folding diseases. Prion 2014; 8.

44. Van Goor F, Hadida S, Grootenhuis PD, et al. Correction of the F508del-CFTR protein processing defect in vitro by the investigational drug VX-809. Proc Natl Acad Sci U S A 2011; 108: 18843-18848.

45. Arbini AA, Mannucci M, Bauer KA. A Thr359Met mutation in factor VII of a patient with a hereditary deficiency causes defective secretion of the molecule. Blood 1996; 87: 5085-5094.

46. Enjolras N, Plantier JL, Rodriguez MH, et al. Two novel mutations in EGF-like domains of human factor IX dramatically impair intracellular processing and secretion. J Thromb Haemost 2004; 2: 1143-1154.

47. Griesemer M, Young C, Robinson AS, et al. BiP clustering facilitates protein folding in the endoplasmic reticulum. PLoS Comput Biol 2014; 10: e1003675.

Figure legends

Figure 1: Reduced FVII:Ag in cell lysates and culture medium from cells expressing rFVII mutants. HEK293 cells were transiently transfected with the constructs pcDNA3-FVIIwt, pcDNA3-p.Q160R, pcDNA3-p.I289del or pcDNA3-p.A354V-p.P464Hfs. 48 h post-transfection FVII:Ag levels were measured by ELISA in cell lysates (black bars) and culture medium (white bars). Relative FVII:Ag levels were calculated by dividing the FVII:Ag level (mU) by the corresponding total protein content in the lysates (µg). The results are presented relative to rFVIIwt levels. Values are mean ± SEM of three individual experiments (n=6, ****p≤0.0001, ***p≤0.001, **p≤0.01, *p≤0.05).

Figure 2: Increased half-lives of rFVII-160R, rFVII-289del and rFVII-354V-464Hfs compared to rFVIIwt. FVII:Ag was measured using ELISA on cell lysates from CHO-K1 cells stably expressing rFVIIwt, rFVII-160R, rFVII-289del or rFVII-354V-464Hfs after treatment with the protein synthesis inhibitor CHX for 0, 4, 8, 16 and 24 h. The results are presented relative to the 0 h time point. Values are mean ± SEM of three individual experiments (n=6).

Figure 3: rFVII-160R, rFVII-289del and rFVII-354V-464Hfs induced ER stress and activation of the UPR. A) HEK293 cells were transiently co-transfected with the Cignal ERSE reporter construct or the negative control construct and the constructs pcDNA3-FVIIwt, pcDNA3-p.Q160R, pcDNA3-p.I289del or pcDNA3-p.A354V-p.P464Hfs. The ratios between firefly and Renilla luciferase were used for normalization. The results have been corrected for background activity represented by the negative control. Fold change in luciferase activity was calculated relative to the pcDNA3-FVIIwt construct. Bars represent

mean ± SEM of three individual experiments (n=18, ****p≤0.0001, ***p≤0.001, **p≤0.01, *p≤0.05). B) HEK293 cells were transiently co-transfected with the Cignal ATF6 reporter construct or the negative control construct and the construct pcDNA3-FVIIwt, pcDNA3-p.Q160R, pcDNA3-p.I289del or pcDNA3-p.A354V-p.P464Hfs. The ratios between firefly and Renilla luciferase were used for normalization. The results have been corrected for background activity represented by the negative control. Fold change in luciferase activity was calculated relative to the pcDNA3-FVIIwt construct. Values are mean ± SEM of three individual experiments (n=18, ****p≤0.0001, ***p≤0.001, **p≤0.01, *p≤0.05). C) BiP and D) phosphorylated eIF2α (p-eIF2α) were assessed by Western blot analysis in lysates from HEK293 cells transiently expressing rFVIIwt (lane 1), rFVII-160R (lane 2), rFVII-289del (lane 3) or rFVII-354V-464Hfs (lane 4). Fold increase of BiP and p-eIF2α levels in cells expressing rFVIIwt, rFVII-160R, rFVII-289del and rFVII-354V-464Hfs are shown as bars representing mean ± SEM of three individual experiments (n=3). Bands representing BiP were quantified and normalized to β-actin. Bands representing p-eIF2α were quantified and normalized to total eIF2α and α-tubulin. The results are presented relative to the rFVIIwt levels. (****p≤0.0001, ***p≤0.001, **p≤0.01, *p≤0.05).

Figure 4: Increased UPR activity in cells expressing FVII mutants. HEK293 cells were transiently transfected with the constructs pcDNA3-FVIIwt, pcDNA3-p.Q160R, pcDNA3-p.I289del or pcDNA3-p.A354V-p.P464Hfs. Cells were harvested 16, 24 and 48 h post-transfection. A) mRNA levels of sXBP1 and uXBP1 were assessed using SYBR green qRT-PCR. B) ATF4, C) GRP94, D) GADD34 and E) CHOP mRNA levels were assessed by Taqman qRT-PCR. Quantitation was performed using the comparative C_T method with GAPDH (SYBR green) or PMM1 (Taqman) as the endogenous control genes and empty vector-transfected cells as the calibrator. Bars represent mean fold-change in expression of

the target gene in rFVII-160R, rFVII-289del or rFVII-354V-464Hfs expressing cells relative to rFVIIwt expressing cells. Each graph shows expression levels at the time-point where target upregulation was the highest: 16 h (uXBP1, sXBP1, GRP94), 24 h (CHOP) and 48 h (GADD34, ATF4) Values are mean ± SEM of at least three individual experiments (n=15, ****p≤0.0001, ***p≤0.001, **p≤0.01, *p≤0.05).

Figure 5: FVII mutants have increased association with ER chaperones. A) HEK293 cells were transiently transfected with the constructs pcDNA3-FVIIwt, pcDNA3-p.Q160R, pcDNA3-p.I289del or pcDNA3-p.A354V-p.P464Hfs. FVII:Ag levels were determined by ELISA and equivalent amounts of FVII from cell lysates were analyzed by SDS-PAGE under non-reducing conditions and immunoblotted with antibody against FVII to detect FVII-chaperone complexes. Similar results were obtained from three individual experiments. The position of FVII complexes are marked with boxes. B) Western blot analysis was performed with antibodies against candidate chaperones Three independent experiments with similar results were performed. Band intensities of complexes from immunoblots probed with antibody against FVII (C), BiP (D) or GRP94 (E) were quantified. Values are mean ± SEM of three individual experiments (n=3, ****p≤0.0001, ***p≤0.001, **p≤0.01, *p≤0.05). F) HEK293 cells were transiently transfected with the constructs pcDNA3-FVIIwt, pcDNA3-p.Q160R, pcDNA3-p.I289del or pcDNA3-p.A354V-p.P464Hfs. The cell lysates were co-immunoprecipitated with anti-FVII antibodies or negative control antibodies. The interacting proteins in co-immunoprecipitations or in the input were examined by Western blot analysis with anti-BiP, anti-GRP94 or anti-FVII antibodies.

Figure 6: UPR inhibition increases intracellular FVII levels. HEK293 cells transiently expressing rFVIIwt, rFVII-160R, rFVII-289del or rFVII-354V-464Hfs were treated with

UPR inhibitors GSKi (A), 4μ8C (B) and AEBSF (C). rFVII:Ag levels in cell lysates were measured by ELISA. Relative rFVII:Ag levels were calculated by dividing the FVII antigen level (mU) by the total protein content in the lysates (μg). The results are presented relative to the non-treated cells. Values are mean ± SEM of three individual experiments (n=6, ****p≤0.0001, ***p≤0.001, **p≤0.01, *p≤0.05).

What is known about this topic?

- Patients with FVII mutations p.Q160R, p.I289del and FVIIp.A354V-p.P464Hfs have low FVII:Ag levels in plasma and manifest with bleeding diathesis.
- The secretory defects seen in patients may be attributable to a misfolding mutant molecule.

What does this paper add?

- *In vitro* expression of the FVII mutants demonstrates reduced secretion and intracellular retention.
- FVII mutants are retained intracellularly due to an excessive binding to chaperones in the ER.
- Intracellular retention causes ER stress and activation of the unfolded protein response, most severe for the p.I289del and the FVIIp.A354V-p.P464Hfs mutants.

Figures

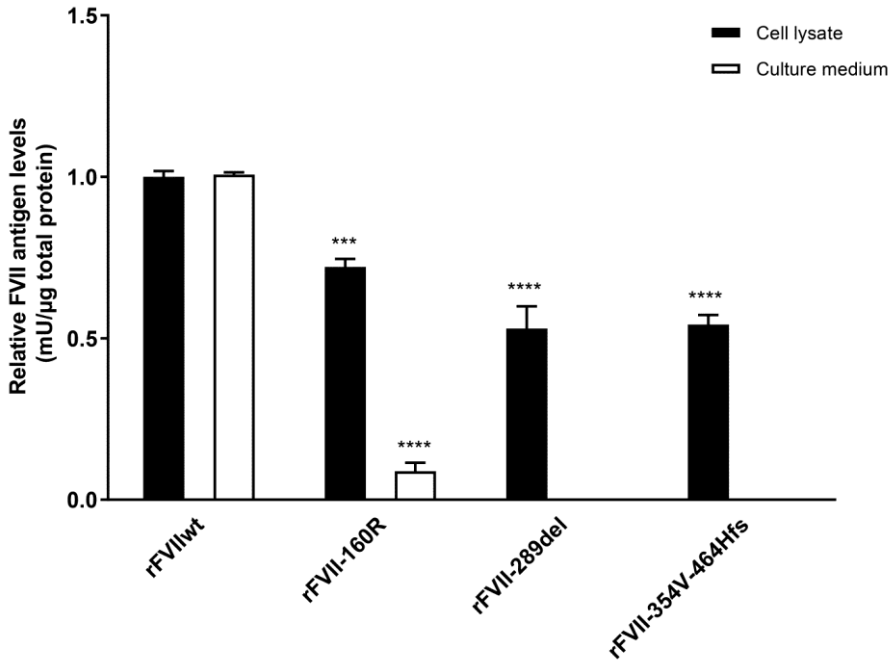

Figure 1

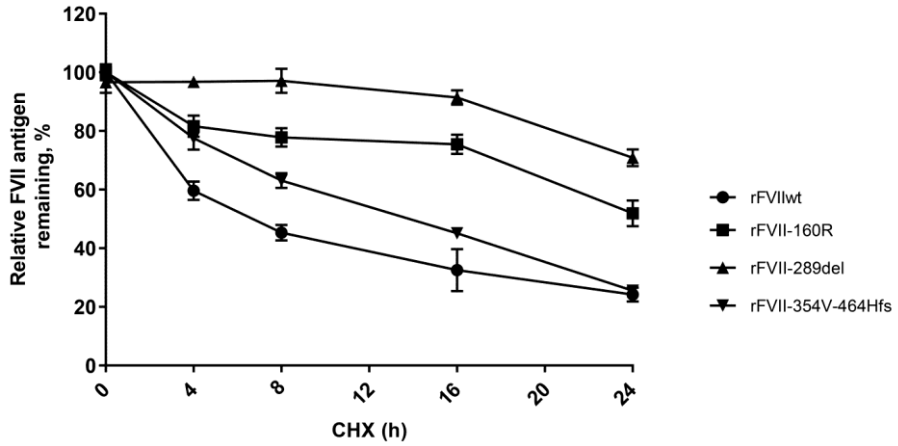
Relative FVII antigen remaining, %
120
100
80
60
40
20
0
0
4
8
12
16
20
24
CHX (h)
rFVIIwt
rFVII-160R
rFVII-289del
rFVII-354V-464Hfs

Figure 2

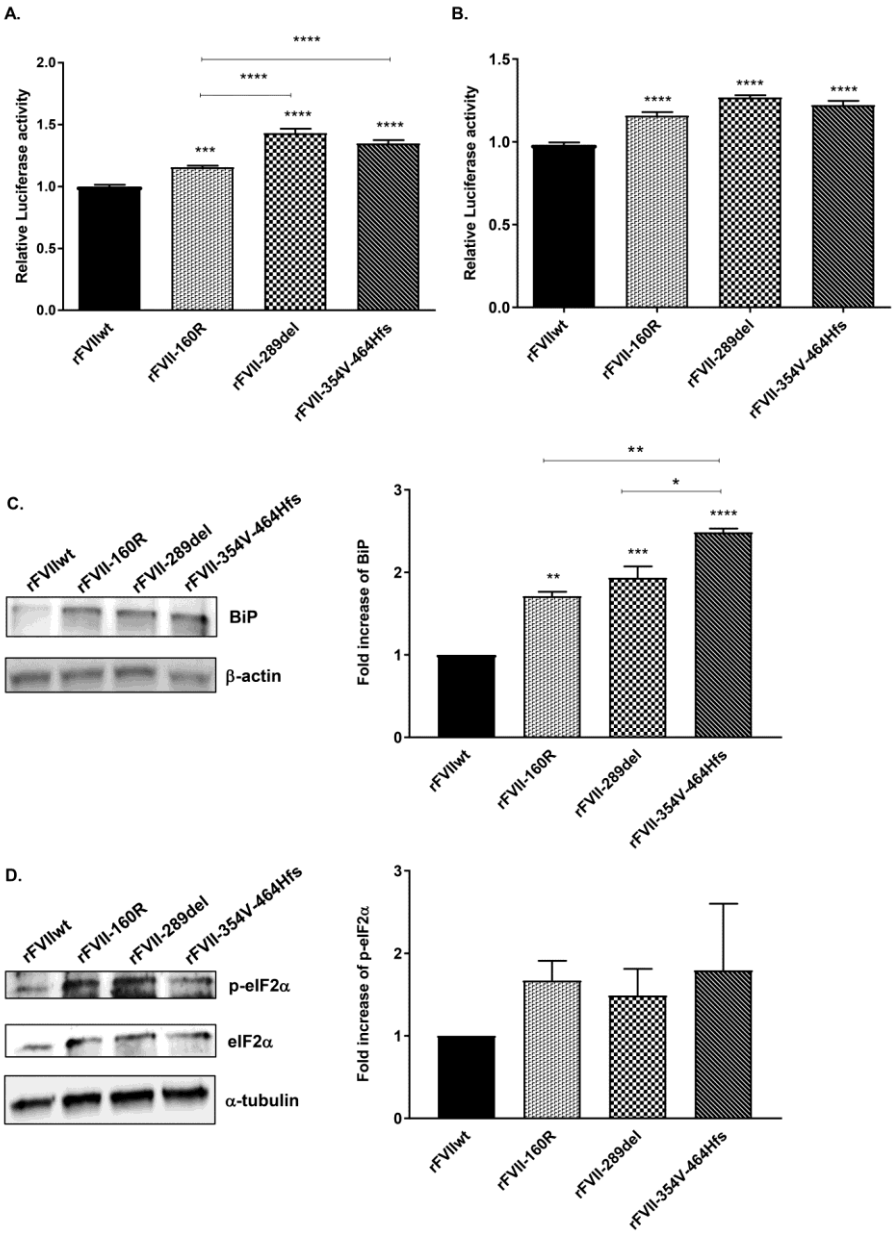
A.
Relative Luciferase activity
2.0
1.5
1.0
0.5
0.0
****
****
****
***
****
rFVIIwt
rFVII-160R
rFVII-289del
rFVII-354V-464Hfs
B.
Relative Luciferase activity
1.5
1.0
0.5
0.0
****
****
****
rFVIIwt
rFVII-160R
rFVII-289del
rFVII-354V-464Hfs
C.
rFVIIwt
rFVII-160R
rFVII-289del
rFVII-354V-464Hfs
BiP
β-actin
Fold increase of BiP
3
2
1
0
**
*
****
**
***
rFVIIwt
rFVII-160R
rFVII-289del
rFVII-354V-464Hfs
D.
rFVIIwt
rFVII-160R
rFVII-289del
rFVII-354V-464Hfs
p-eIF2α
eIF2α
α-tubulin
Fold increase of p-eIF2α
3
2
1
0
rFVIIwt
rFVII-160R
rFVII-289del
rFVII-354V-464Hfs

Figure 3

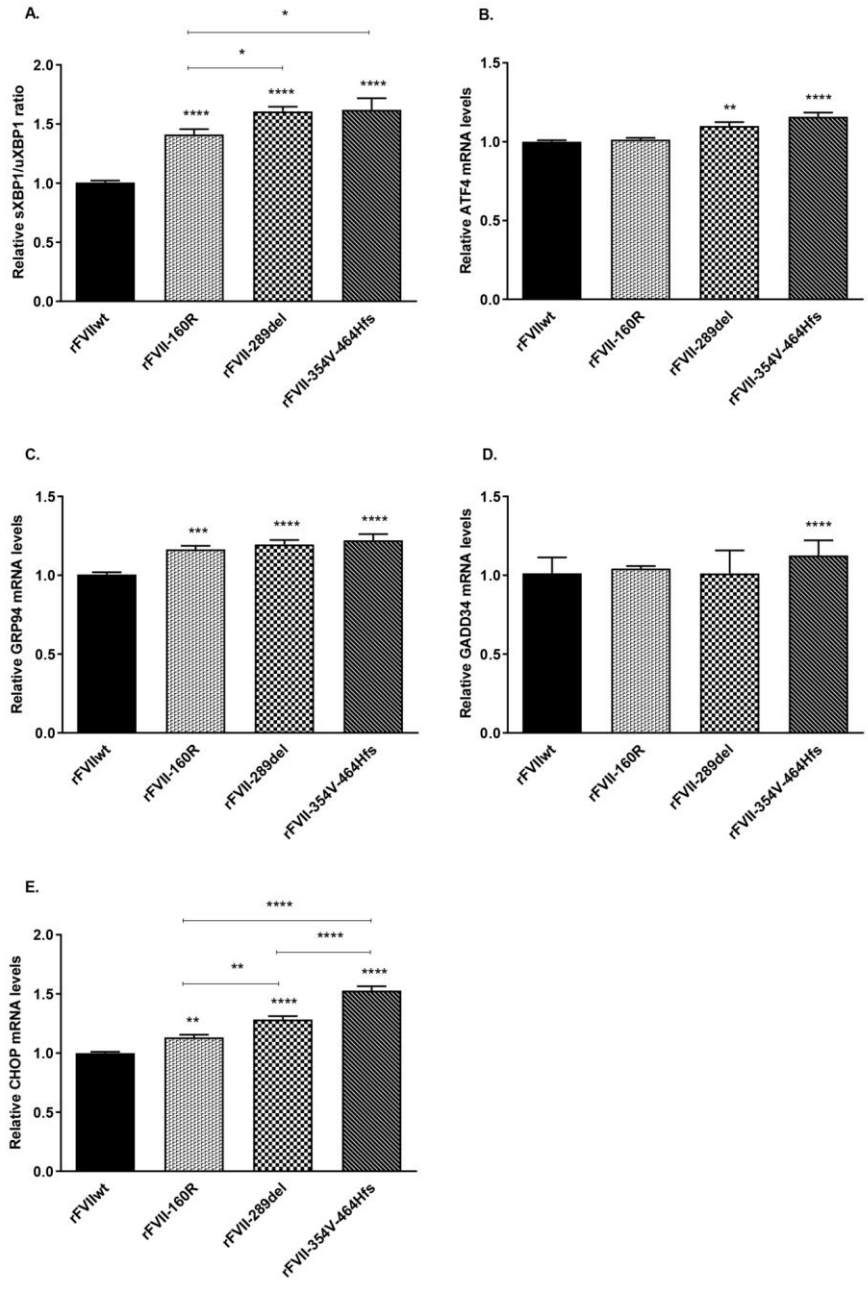
A.
Relative sXBP1/uXBP1 ratio
2.0
1.5
1.0
0.5
0.0
*
*
****
****
****
rFVIIwt
rFVII-160R
rFVII-289del
rFVII-354V-464Hfs
B.
Relative ATF4 mRNA levels
1.5
1.0
0.5
0.0
**
****
rFVIIwt
rFVII-160R
rFVII-289del
rFVII-354V-464Hfs
C.
Relative GRP94 mRNA levels
1.5
1.0
0.5
0.0
***
****
****
rFVIIwt
rFVII-160R
rFVII-289del
rFVII-354V-464Hfs
D.
Relative GADD34 mRNA levels
1.5
1.0
0.5
0.0
****
rFVIIwt
rFVII-160R
rFVII-289del
rFVII-354V-464Hfs
E.
Relative CHOP mRNA levels
2.0
1.5
1.0
0.5
0.0
****
****
**
**
****
****
rFVIIwt
rFVII-160R
rFVII-289del
rFVII-354V-464Hfs

Figure 4

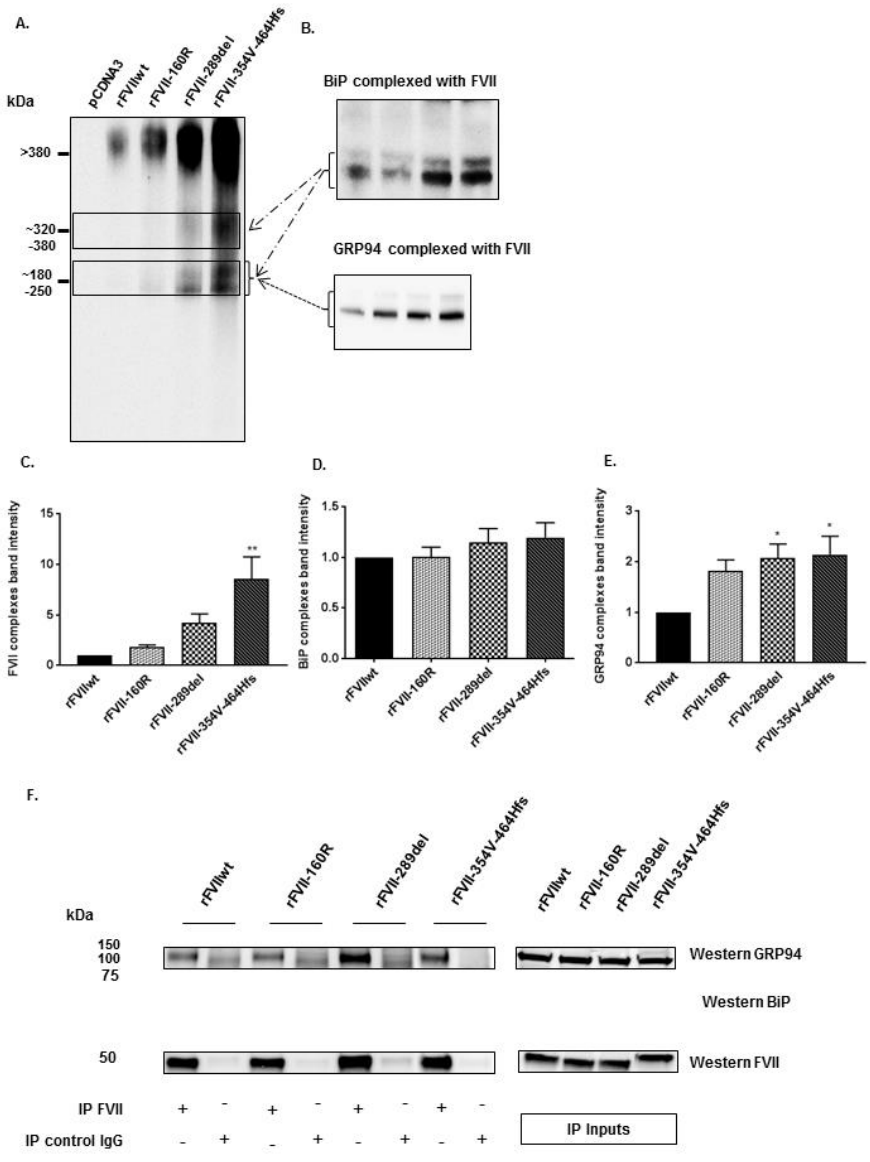

Figure 5

Commentato [EA4]: Preliminary figure 5F (missing pictures of BiP and the ladder).

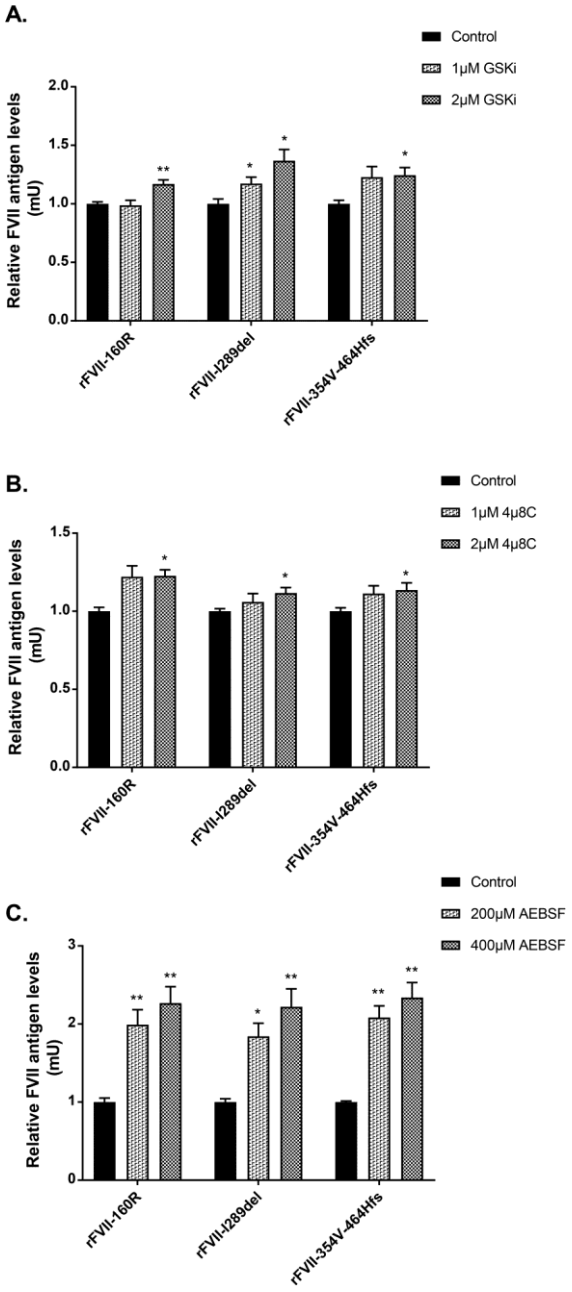
A.
Control
1μM GSKi
2μM GSKi
Relative FVII antigen levels (mU)
2.0
1.5
1.0
0.5
0.0
**
*
*
*
rFVII-160R
rFVII-I289del
rFVII-354V-464Hfs
B.
Control
1μM 4μ8C
2μM 4μ8C
Relative FVII antigen levels (mU)
1.5
1.0
0.5
0.0
*
*
*
rFVII-160R
rFVII-I289del
rFVII-354V-464Hfs
C.
Control
200μM AEBSF
400μM AEBSF
Relative FVII antigen levels (mU)
3
2
1
0
**
**
*
**
**
**
rFVII-160R
rFVII-I289del
rFVII-354V-464Hfs

Figure 6